37th International Astronautical Congress. Innsbruck, Austria.
Oct 4-11, 1986. Paper IAF-86-268.

8. THE MICROGRAVITY ENVIRONMENT OF THE D1 MISSION

H. HAMACHER[1], U. MERBOLD[2], R. JILG [1]
[1] Deutsche Forschungs- und Versuchsanstalt für Luft- und Raumfahrt e.V. (DFVLR), Köln, FRG
[2] European Space Agency (ESA), Paris, France

Abstract

Some characteristic features and results of D1 µg-measurements are discussed as performed in the Material Science Double Rack and MEDEA. Starting with a brief review of main potential disturbances, the payload aspects of interest to the analysis and the accelerometer measuring systems are described. The µg-data are analysed with respect to selected mission events such as thruster firings for attitude control, operations of Spacelab experiment facilities, vestibular experiments and crew activities. The origins are divided into orbit, vehicle, and experiment induced perturbations. It has been found that the µg-environment is dictated mainly by payload-induced perturbations. To reduce the µg-level, the design of some experiment facilities has to be improved by minimizing the number of moving parts, decoupling of disturbing units from experiment facilities, by taking damping measures, etc. In addition, strongly disturbing experiments and very sensitive investigations should be performed in separate mission phases.

1. Introduction

The Spacelab Mission D1 was primarily dedicated to carry out experiments which made use of the low level of gravitation aboard an orbiting spacecraft. Although reduced by several orders of magnitude compared to 1g on ground, the residual microgravity (μg-)level still affects physical processes in very individual ways [1]. Hence, the knowledge of the actual μg-environment during the processing time is an important basis for the final scientific analysis of the results. In contrast to the steady-state gravitational field on earth, the μg-vector field aboard a spacecraft is characterized (i) by a steady-state dc component and (ii) by a fluctuating ac contribution called g-jitter, being inherently local and statistical in nature with peak values usually far above the level of the dc component.

To measure the microgravity history achieved during D1, various payload elements were equipped with accelerometer packages. Figure 1 shows on the starboard and the portside of the payload locations and measurement axis of the accelerometers installed [2]. The knowledge of the actual μg-environment is also an important basis to examine and improve the design and operational concept of the payload.

In this paper characteristic features and results of μg-measurements are presented as performed in the Material Science Double Rack (MSDR) and in MEDEA. Starting with a brief review of main potential disturbances, the payload aspects of interest to the analysis and the accelerometer measuring systems will be described. This is followed by the discussion of μg-data with respect to their potential causes.

2. Causes of Main Disturbances

It is one of the unique possibilities of space flight that a freely orbiting spacecraft offers a virtually zero-gravity state to its interior objects without time limitations by trajectory kinematics. For the spacecraft center of mass (CM), the gravitational force is balanced by the centrifugal force. Zero gravity, however, is an ideal state that cannot be accomplished completely in a real spacecraft due to a number of deviations from the model of a freely drifting mass point. The residual μg vector field may be described by

$$\vec{a} = \Sigma \, (\vec{a}_s + \vec{a}_{tr})$$

where $\vec{a}_s$ and $\vec{a}_{tr}$ are a quasi steady and a transient vector, respectively. $\vec{a}_s$ has a frequency typical of the order of the orbital frequency. $\vec{a}_{tr}$ is characterized by a wide spectral range of frequencies large in comparison with that of $\vec{a}_s$.

2.1 Quasi Steady Accelerations

2.1.1 Atmospheric Drag

Due to e x t e r n a l forces, mainly the residual atmospheric drag, the orbiter is not in a freely drifting state, giving rise to a quasi s t e a d y acceleration a_d of the CM, acting opposite to the orbital velocity vector [3]. The level of a_d versus altitude as predicted for various orbiter flight modes is depicted in Fig. 2. For the D1 nominal flight altitude of 324 km, a maximum of $a_d \cong 1 \cdot 10^{-6} g_o$ (g_o = 9.81 ms^{-2} the gravitational acceleration on ground) is expected for the flight mode with the largest projected cross-sectional area [4]. As a result of the atmospheric density variations along one orbit there is always a pulsation of twice the orbital frequency [5].

2.1.2 Gravity Gradient Effects

For objects located off CM gravity and centrifugal forces are no longer balanced completely, giving rise to a "tidal acceleration" a_t which is proportional to the displacement r from CM (Fig. 3). In case of 324 km altitude and Gravity Gradient Mode yields [3]

$$a_t = 1.36 \cdot 10^{-7}\ g_o\ [m^{-1}] \begin{pmatrix} 0 & 0 & 0 \\ 0 & -1 & 0 \\ 0 & 0 & 3 \end{pmatrix} \begin{pmatrix} x \\ y \\ z \end{pmatrix}$$

Figure 4 shows the location of the MSDR and MEDEA with respect to the total CM. Based on a typical displacement of $r \leq 2{,}5$ m it may be stated that a_t is always below $10^{-6}\ g_o$.

2.1.3 Orbiter Rotation

Orbiter rotation for attitude changes were performed by rotation rates $\omega_r \leq 0.2$ deg/sec, resulting in a centrifugal acceleration at r = 2.5 m of

$$a_c = r\omega_r^2 \leq 3.1 \cdot 10^{-6} g_o.$$

This steady acceleration $\vec{a}_c$ is always superimposed by the tidal vector $\vec{a}_t$ which rotates relative to $\vec{a}_c$ by $2 \cdot \vec{\omega}_r$. The magnitude of the quasi steady vectors are depicted in the g/g_o vs frequency plot Fig. 5. It follows that the magnitude of $\vec{a}_c$ may exceed both the drag and the tidal acceleration. The only existing measurement value of the quasi steady component results from an analysis of the path of a freely floating particle. It was recorded by the Fluid Experiment System FES during SL-3 [5]. This value conforms fairly well with the predictions of drag and tidal acceleration.

2.2 Transient Accelerations

A variety of transient external and internal forces give causes to transient accelerations, resulting in exitations of the spacecraft flexibility modes. The induced g-j i t t e r are characterized by a wide frequency spectrum. Transient e x t e r n a l forces may result from operational activities, such as thruster firings for attitude control and extra vehicular activities. These forces in general exert also a torque to the vehicle, resulting in a transient rotational acceleration phase and followed by a quasi steady acceleration period due to a constant rotation around CM.

The mass allocation inside a spacecraft is changing due to the motion of mechanical parts, crew activities, etc., giving rise to i n t e r n a l forces. These forces do not involve a momentum change to the spacecraft CM system. Impulses caused by internal forces are always compensated by equal and opposite impulses with a time delay. Even though the induced g-jitter may reach high peak values, the resulting displacement of particles with respect to the CM is small because of its compensated and random nature.

3. Acceleration Monitoring Systems

The analysis presented in this paper is based on data of the MSDR package and the three-axis sensor of MEDEA (Fig. 1). The technical data are listed in Table 1 [5]. The detection range covered by these systems are indicated in Fig. 5. It may be seen that none of the systems is suited to detect the steady state component.

Table 1: Technical Data of the D1 Accelerometer Systems [2]

	MSDR	MEDEA[1)]
Measurement axis	u, v, w	x, y, z
Detection mode	peak detection	equally spaced time axis
Sampling rate, Hz	1	107
Range, mg	10^{-2} - 10	10^{-1} - 100
Resolution, mg	10^{-3}	$5 \cdot 10^{-2}$
Band width, Hz	0 - 100	0 - 10

1) High Precision Thermostat (HPT) package

The MSDR accelerometer was operated in a peak detection mode to reduce the total amount of data. Peak values within intervals of Δt = 1 sec were detected from an analogue random response in positive and negative direction of the coordinate considered (Fig. 6). The resulting step functions a are the envelopes of the analogue signal. Figure 7 shows a typical reading of the MSDR system. The lowest value detectable by peak detection is determined (i) by periodic vibrations having frequencies higher than the sampling rate, (ii) by steady accelerations and (iii) by a zero point offset. As a result, the data recorded by peak detection do not allow for zero point corrections, calculation of the resultant acceleration vector, and any frequency analysis.

The MEDEA package was operated in a high rate sampling mode, suited to perform frequency analysis up to about 5 Hz.

4. Data Analysis

In the following, examples of different classes of disturbances will be discussed with respect to their causes as identified by correlation with the mission timelines and onboard video recordings. The examples are subdivided into vehicle and experiment induced perturbations, the latter also including those originating from crew activities.

4.1 Orbiter Induced Disturbances

The first series of measurements are orbiter-induced perturbations caused by firing the different thruster systems. Figure 8 shows a MSDR reading taken during the firing of the Vernier Thruster System (VRCS), being part of the Reaction Control System (RCS). The Vernier Thrusters serve to initiate and to stop orbiter rotation for attitude changes. The spikes induced are of the order of 1 mg. The number of attitude maneuvers necessary during a mission depends on the kind of experiments aboard Spacelab. In a microgravity oriented mission the orbiter is flown preferably in the gravity gradient stabilized attitude with a minimum of thruster firings needed. As given in the as-flown timeline of D1 [6], 29 % of the SL-activated time have been flown in the Gravity Gradient Mode within five time phases lasting between 7 1/2 and 12 hours each. The comparison with SL-1 with 4 % in Gravity Gradient Mode reflects the µg-dedicated character of D1 and the multidisciplinary nature of SL-1.

The second group of thrusters incorporated in the RCS are the Primary Thrusters (PRCS) utilized for velocity changes, docking maneuvers, etc. Firings of the PRCS are rather rare events during a mission. Figure 9 shows the test firing prior to the descent as recorded by the MEDEA system. This series of firings shows highest spikes in z-direction (60 mg) and a decay time of the structural vibration as long as about 11 sec.

4.2 Disturbances by Experiment Operations

The second group of perturbations analysed in this paper are those caused by the payload itself. Starting with vestibular experiments, MSDR perturbations and crew activities will be discussed.

4.2.1 Vestibular Experiments

Vestibular experiments frequently have strong effects on the µg level [7]. Severe disturbances have been detected during the "Hop and Drop" experiments. One of the science astronauts was jumping along the positive z-coordinate while "hopping" and was pulled down to the Spacelab floor by elastic cords. Figure 10 is the time history of a "hop" series as recorded in MEDEA. The dominating response is in the z-axis which was the jump direction. An effective tool for discussing the signals are the corresponding power spectral density (PSD) functions describing the power distribution over the time history of fig. 10. The peak at 1.7 Hz in the z-plane represents the "hop" frequency. The dominating peak at 5 Hz, appearing in all coordinates, indicates the eigenfrequency of the Spacelab module in its suspension.

The second part of this experiment was the "drop" exercise. It was started from a holding of the science astronaut on the upper part of a SL-rack. After the release he was pulled down to the floor by the cords. The time history of a series is depicted in Fig. 12, showing decay times of the order of 6 sec. In the corresponding PSD functions (Fig. 12) a second dominating spike appears between 7 and 8 Hz, which is the eigenfrequency of the rack row in the suspension, excited by the hold of the astronaut.

A second example is the Vestibular Sled Facility consisting of a motor-driven seat and a 4 m runway which is fixed in the Spacelab aisle. Numerous profiles of acceleration to the test person have been carried out, as for example sinusoidal or trapeziform. A record taken in MEDEA during trapeziform acceleration of 200 mg maximum is shown in Fig. 14. The ramp in the x-axis of 0.28 mg average corresponds well to the calculated value for the rigid case. It is interesting to note that the structural vibrations in z-axis exceed temporary x-axis level.

4.2.2 MSDR-Induced Disturbances

Operations of experiment facilities and auxiliary equipment installed in the MSDR naturally have a strong impact on the μg-level detected by the MSDR package. The Fluid Physics Module FPM has been selected as an example to demonstrate the consequences of both the design concept and the operation of a facility on the μg-environment. The FPM induced g-jitter during the operation of rotating and vibrating parts, handling of samples, film changes, etc. For the latter acitivities, the FPM had to be extracted from the rack on telescopic slides. Figure 15 shows a sequence of FPM-induced perturbations. In the first phase, the facility was extracted causing spikes up to full scale. This was followed by a handling period and an operation phase in the oscillation mode generating a relatively uniform pattern. The record taken during the same time phase by the MEDEA system is shown in Fig. 16. Many FPM-induced spikes of the MSDR plot can be correlated with the MEDEA readings. Few of them are indicated by the arrows in Figures 15 and 16.

4.2.3 Crew Activities

From a detailed analysis of the D1 flight video tapes numerous spikes have been identified as a result of crew activities. Two examples are shown in Fig. 17. The spikes exceeding full scale of a_u were generated by closing a container door located in the Spacelab ceiling. The second group of peaks resulted from a Science Astronaut holding to and working at the extracted FPM.

4.2.4 Quiet Phases

The examples discussed are primarily strong disturbing events which are by no means representative for the entire mission. A quiet period, standing for many others of the mission, is shown in Fig. 18 in terms of the magnitude of the resulting vector calculated from MEDEA data.

5. Summary and Discussion

The results of the analysis have been summarized in the g vs f-plot of Fig. 19. Also indicated is the microgravity level recommended for the US Space Station (SS) [3]. In the quasi-steady regime the Spacelab data of the non-rotating case are below the SS requirements [FES, SL-3].
The high frequency regime regime is determined by perturbations generated during the operation of the payload itself with the exception of the PRCS firings which were rather rare events during D1. It may be seen from Fig. 19 that the μg quality can be improved by shifting the vestibular experiments to separate mission phases outside the processing time of sensitive experiments. To further reduce the μg-level, various precautions are possible and necessary. The design concept of some experiment facilities, e.g. the FPM, has to be changed drastically by minimizing the number of moving parts during operation and handling, decoupling of disturbing units (motors, fans) from experiment facilities, by taking damping measures, etc. Moreover, the Science Astronauts should be trained in causing as little accelerations as possible. Another fact, the need for dedicated missions, has been discussed frequently in the past. The D1 Mission was a step in this direction.

In addition to the design and operational precautions, the μg measuring technique aboard Spacelab has to be improved. The peak detection method allows the analysis of transient contributions to the g-jitter and a correlation to their origins. Steady state contributions, however, are hard to identify. This method also suffers from the disadvantage that a possible zero point offset of the system cannot be observed and eliminated from the μg-data,and any frequency analysis is not possible.

Acknowledgement

The authors are indebted to Dr. N. Trappen of DFVLR for his valuable support in processing the μg-flight data.

References

[1] R.J. Naumann, "Susceptibility of Materials Processing Experiments to Low-Level Accelerations", NASA Conf. Publ. 2199 (1981), pp. 63-68

[2] - "Microgravity Environment Acceleration Monitoring Systems of D1-Payload Elements", MBB/ERNO, D1-IN-TN-139-ER (1983).

[3] H. Hamacher, "Simulation of Weightlessness", in "Materials Sciences in Space", edited by B. Feuerbacher, H. Hamacher, R.J. Naumann, Springer (1986), pp 31-51

[4] - "Spacelab Payload Accommodation Handbook", NASA, SPL/2104, Main Vol., Issue 2, Revision 0 (1985)

[5] - "Low Acceleration Characterization of Space Station Environment", Teledyne Brown Engineering, Huntsville (AL), Sp 85-2928, Final Report, Revision B (1985).

[6] - "D1 Timeline As Flown", DFVLR, D1-OP-TN-012-RF (1986).

[7] H. Hamacher, U. Merbold, "The Microgravity Environment of the Materials Science Double Rack During Spacelab-1", Proc. of the AIAA Shuttle Environment and Operations II Conference, Houston, TEX., 13-15 Nov.1985, pp. 228-238.

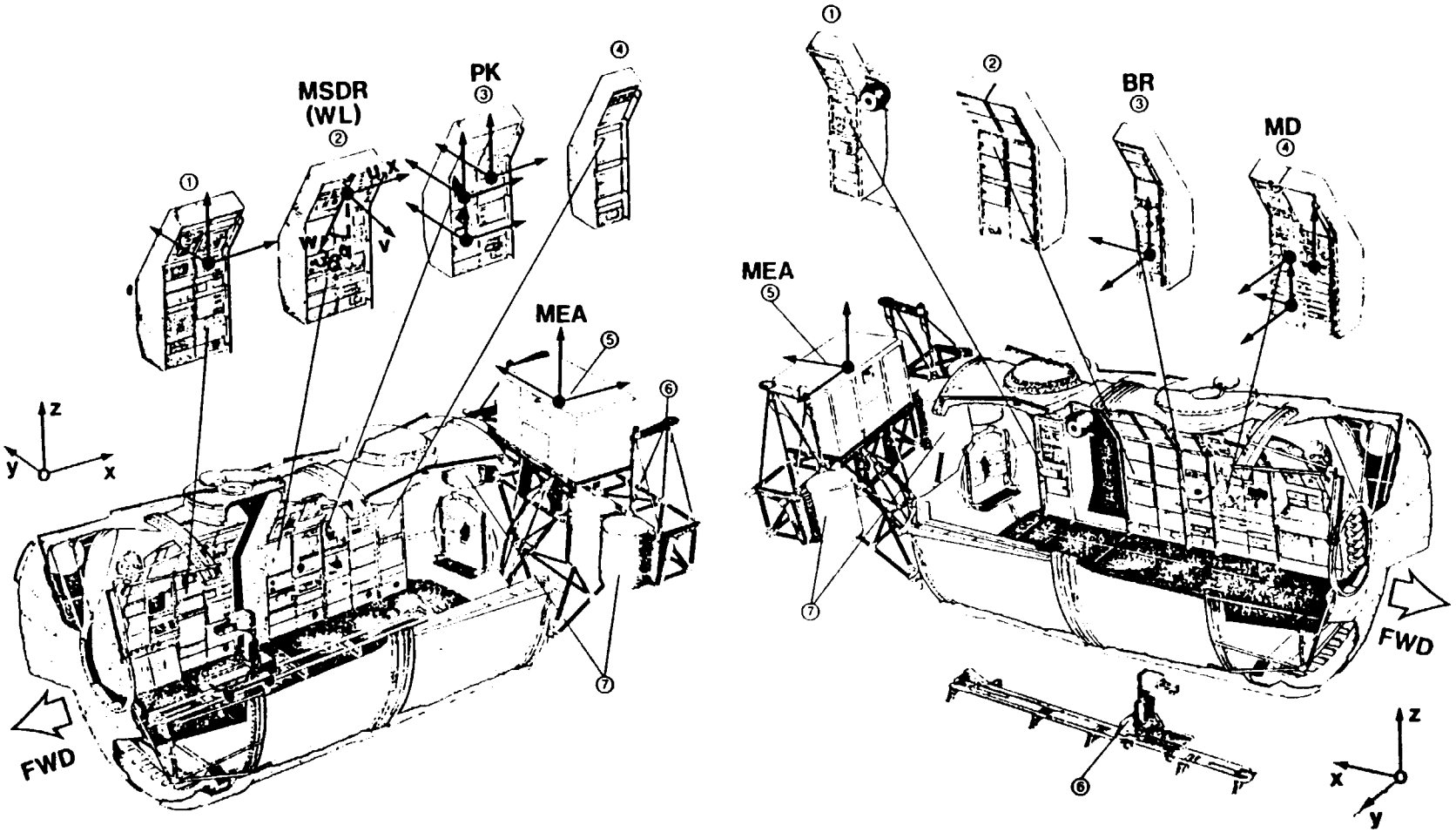

Fig.1. Locations and measurement axis of the accelerometer packages of the D1 payload [2].

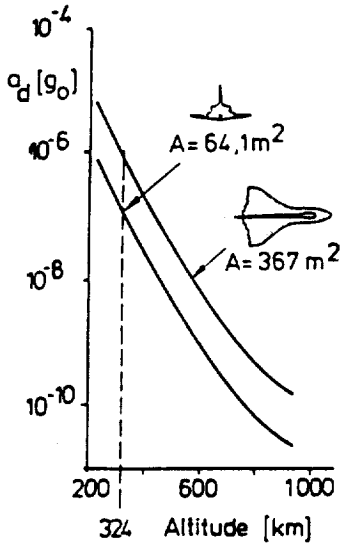

Fig.2.
Calculated effects of atmospheric drag on the Orbiter, m=90718 kg [4].

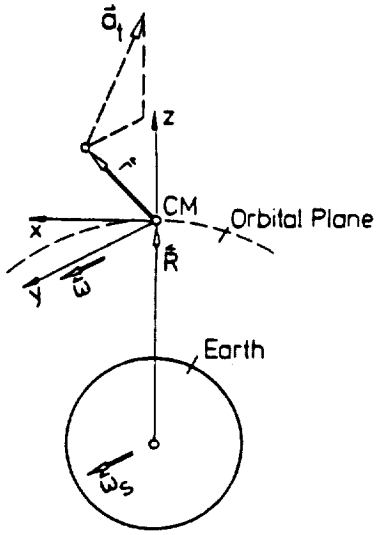

Fig.3.
Definition of the tidal acceleration $\vec{a}_t$.

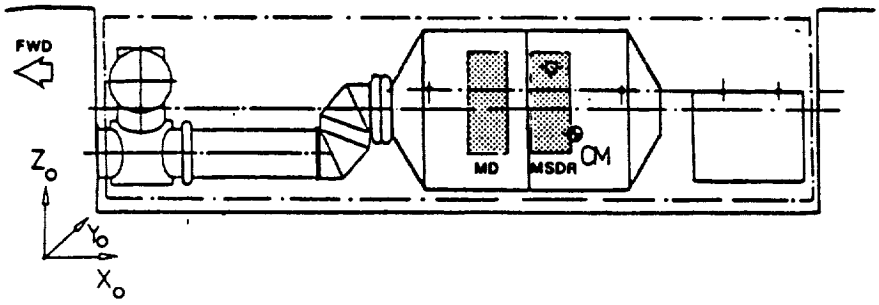

Fig.4. Location of MSDR and MEDEA (MD) relative to the total center of mass (CM).

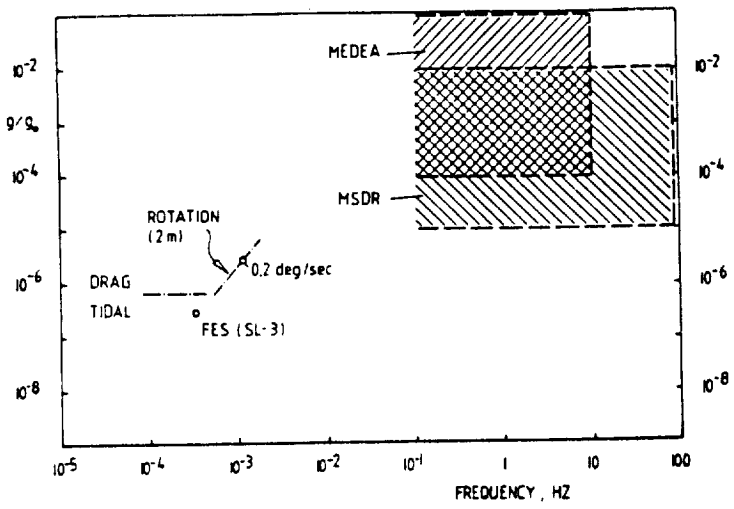

Fig.5.
Measurement range of the MSDR and MEDEA systems.
Quasi-steady components of the Orbiter.

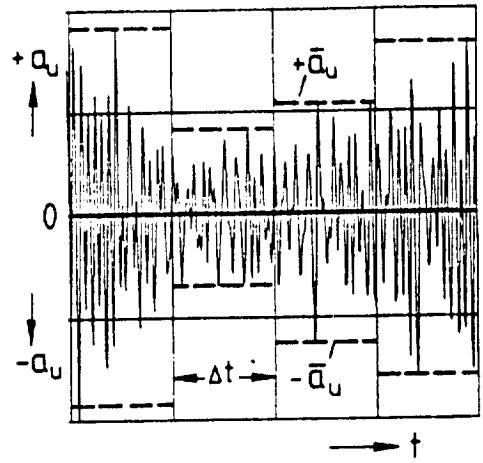

Fig.6.
Illustrating the principle of the peak detection method. The maximum amplitudes within Δt are detected from an analog signal for each direction.

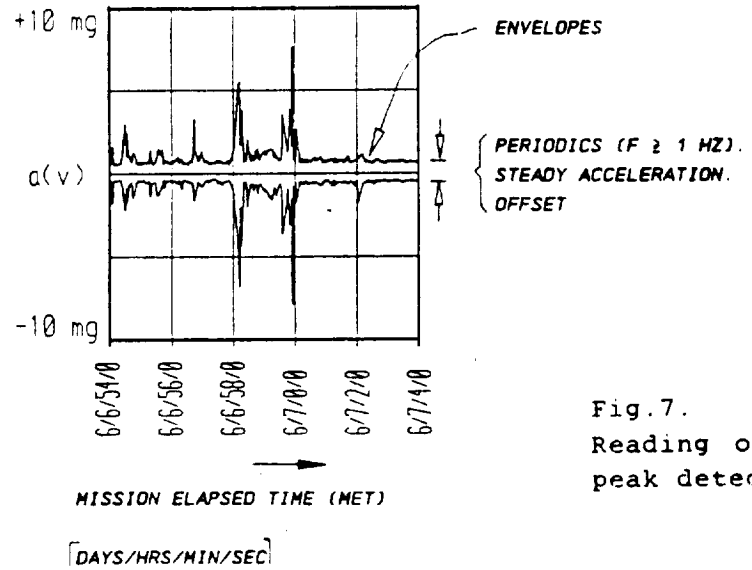

Fig.7.
Reading of the MSDR system in peak detection mode.

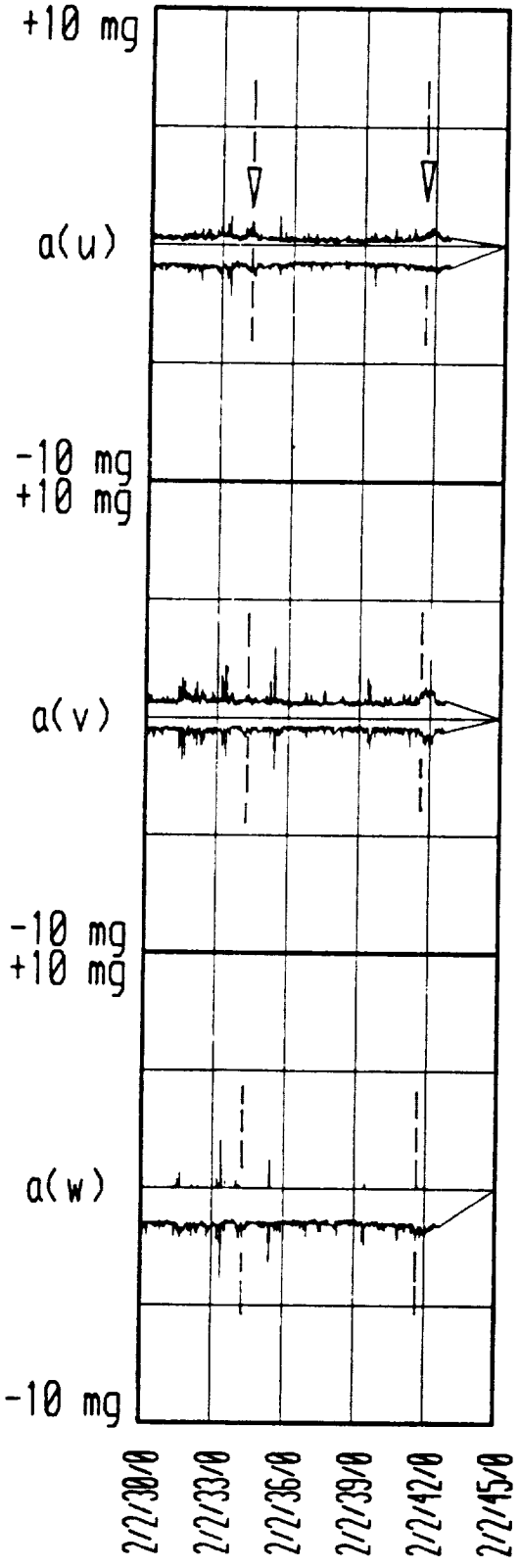

Fig.8.
Two RCS Vernier Thruster firings indicated by arrows (MSDR).

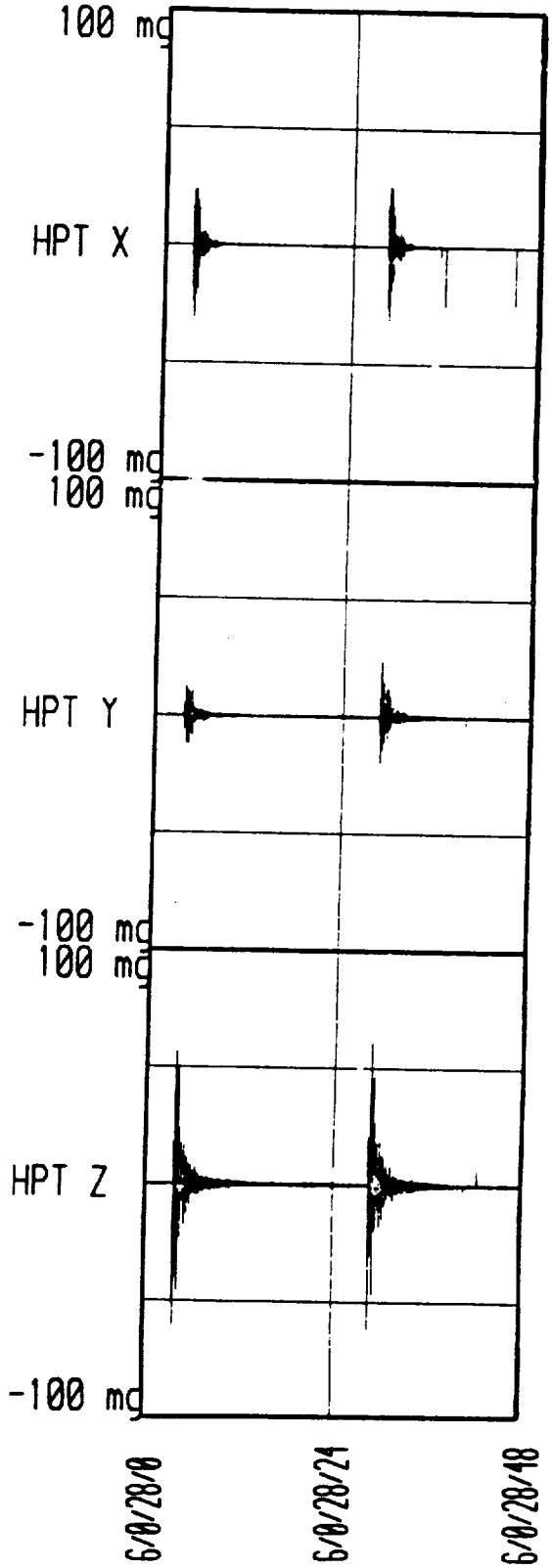

Fig.9.
Two RCS Primary Thruster firings (MEDEA).

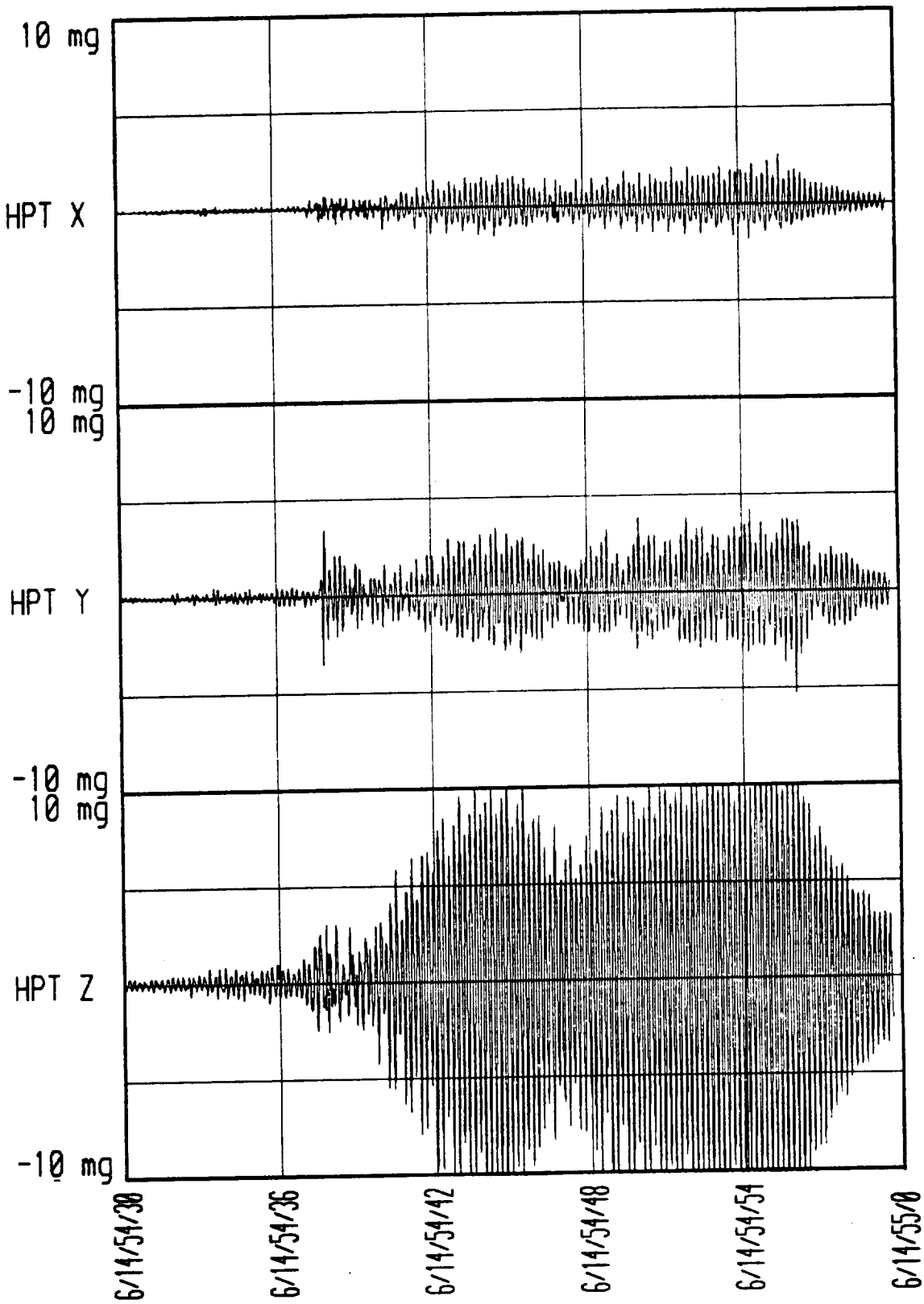

Fig.10. Time history of the "Hop and Drop" experiment, "Hop" phase (MEDEA).

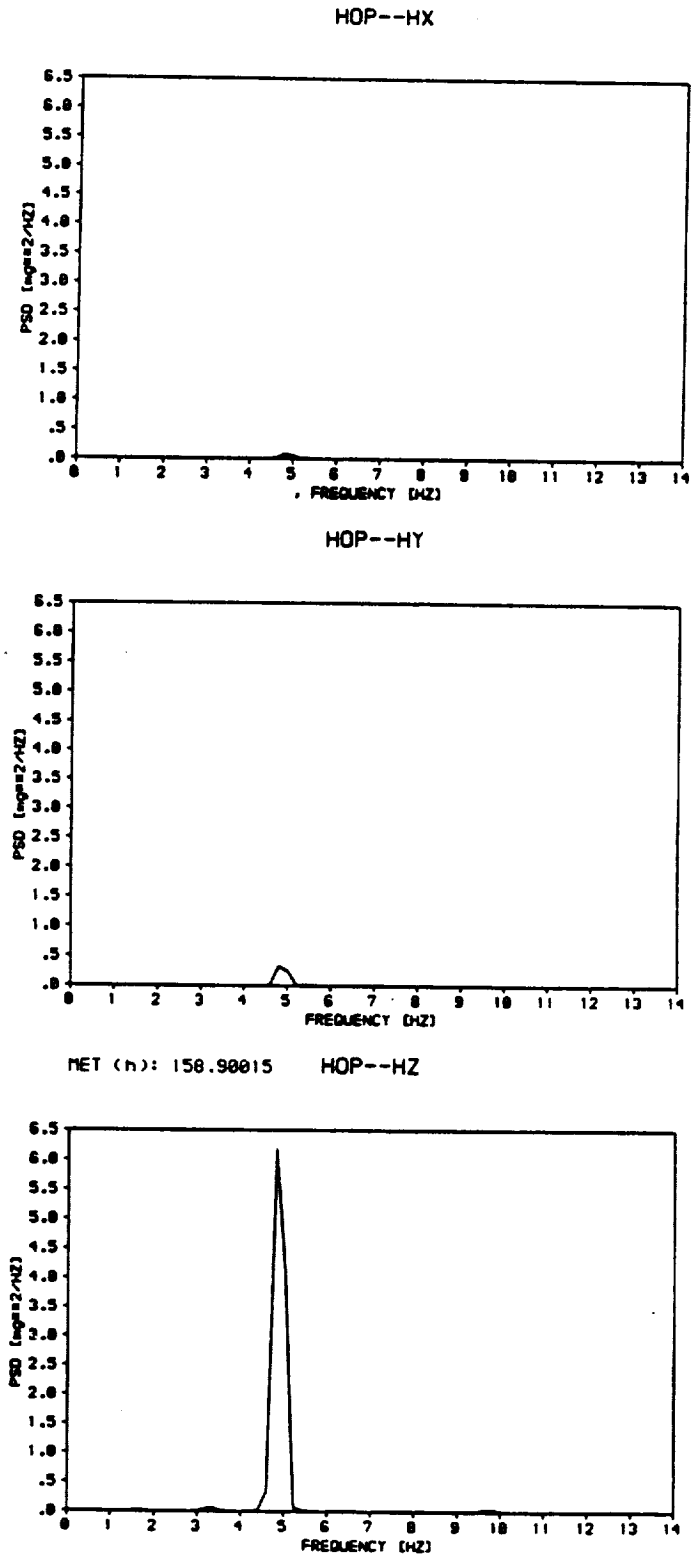

Fig.11. Power spectral density function of "Hop" phase (Fig. 10.).

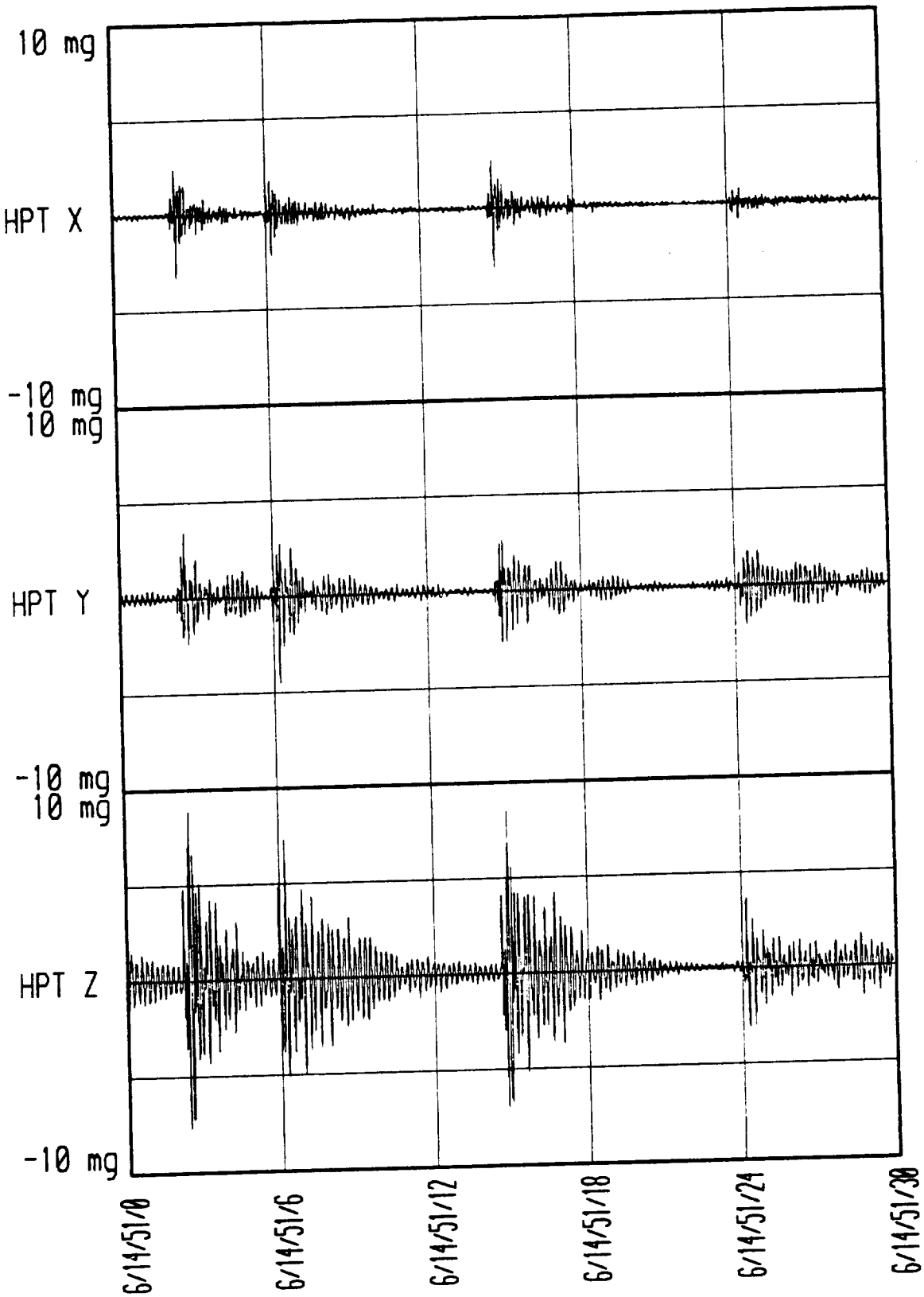

Fig.12. Time history of the "Hop and Drop" experiment, "Drop" phase (MEDEA)

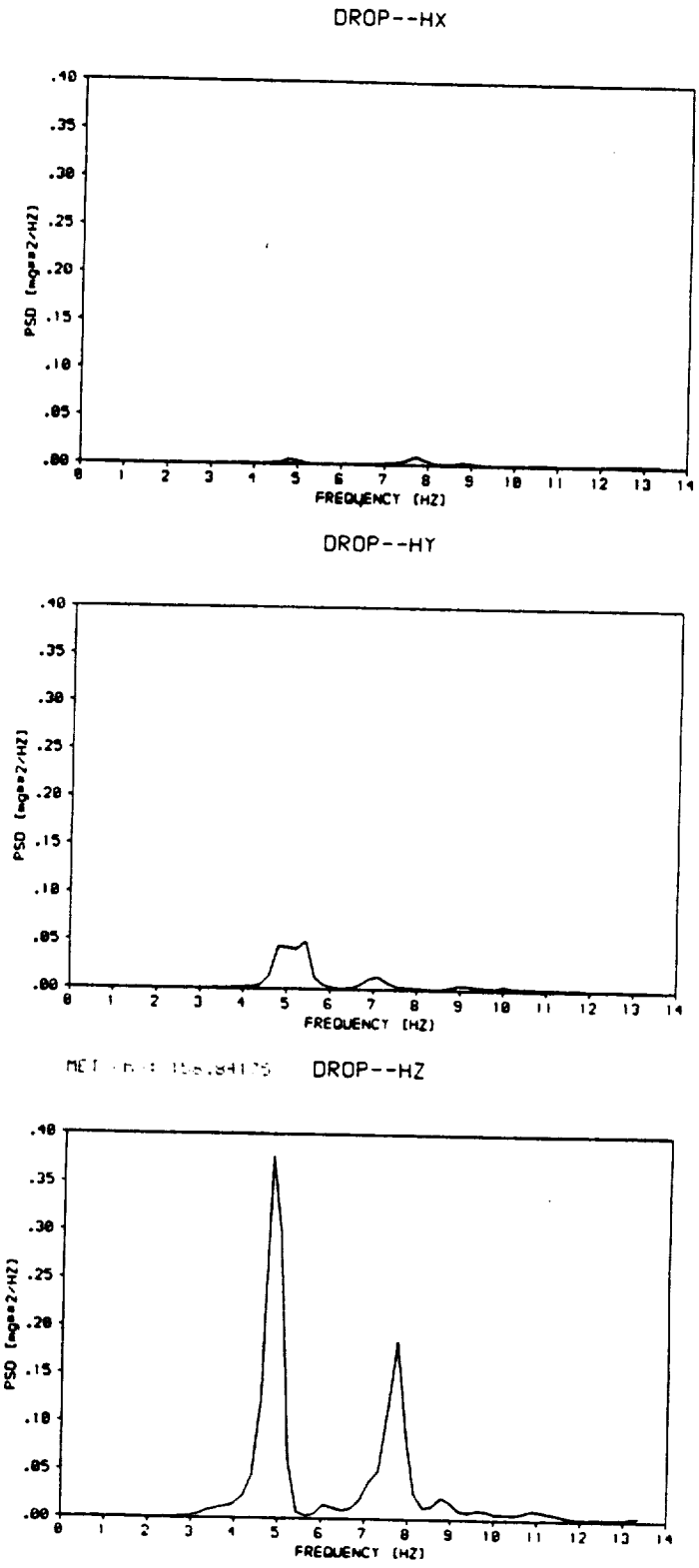

Fig.13. Power spectral density function of "Drop" phase (Fig.12).

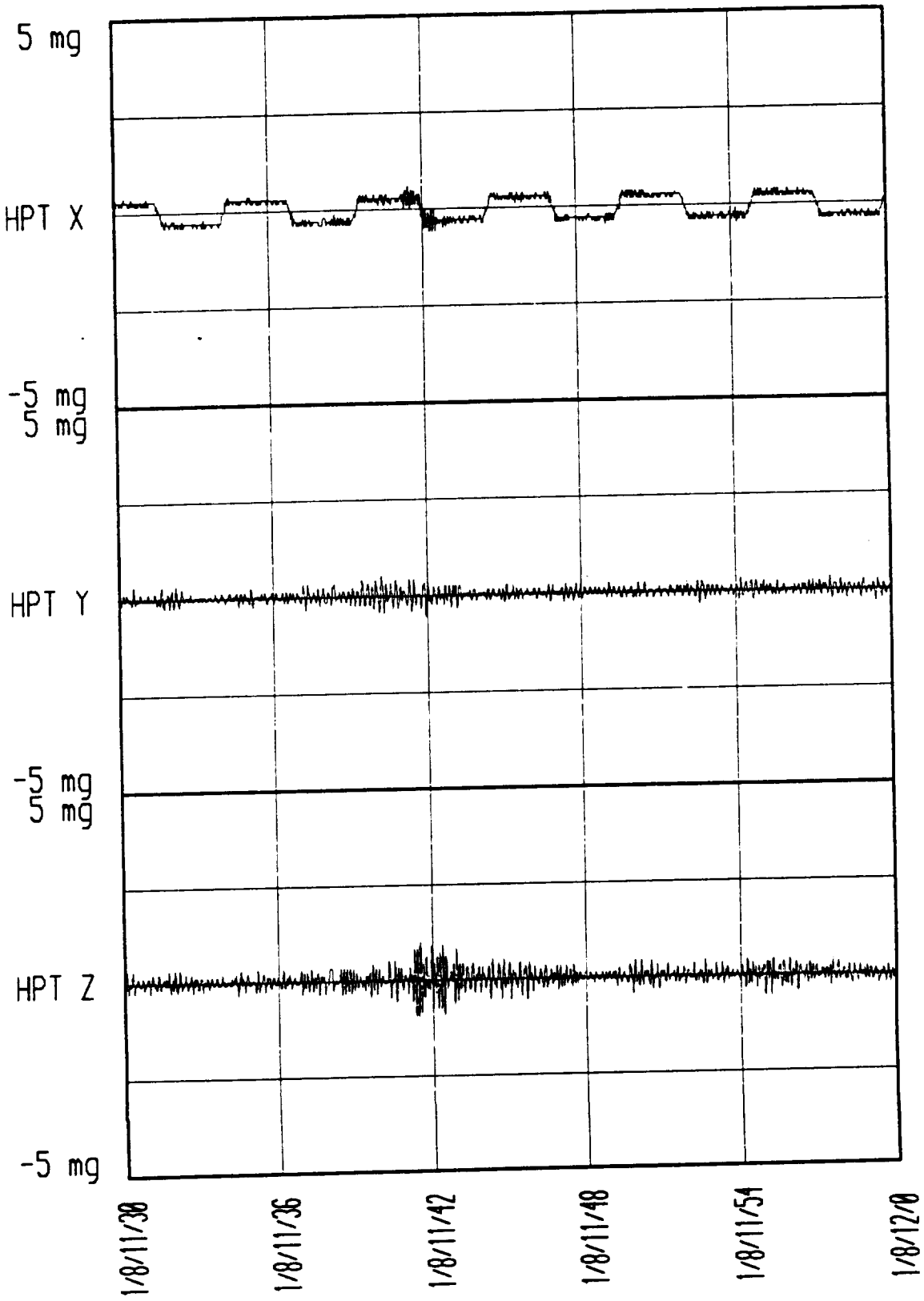

Fig.14. Time history of a Sled run in the trapeziform operation mode.

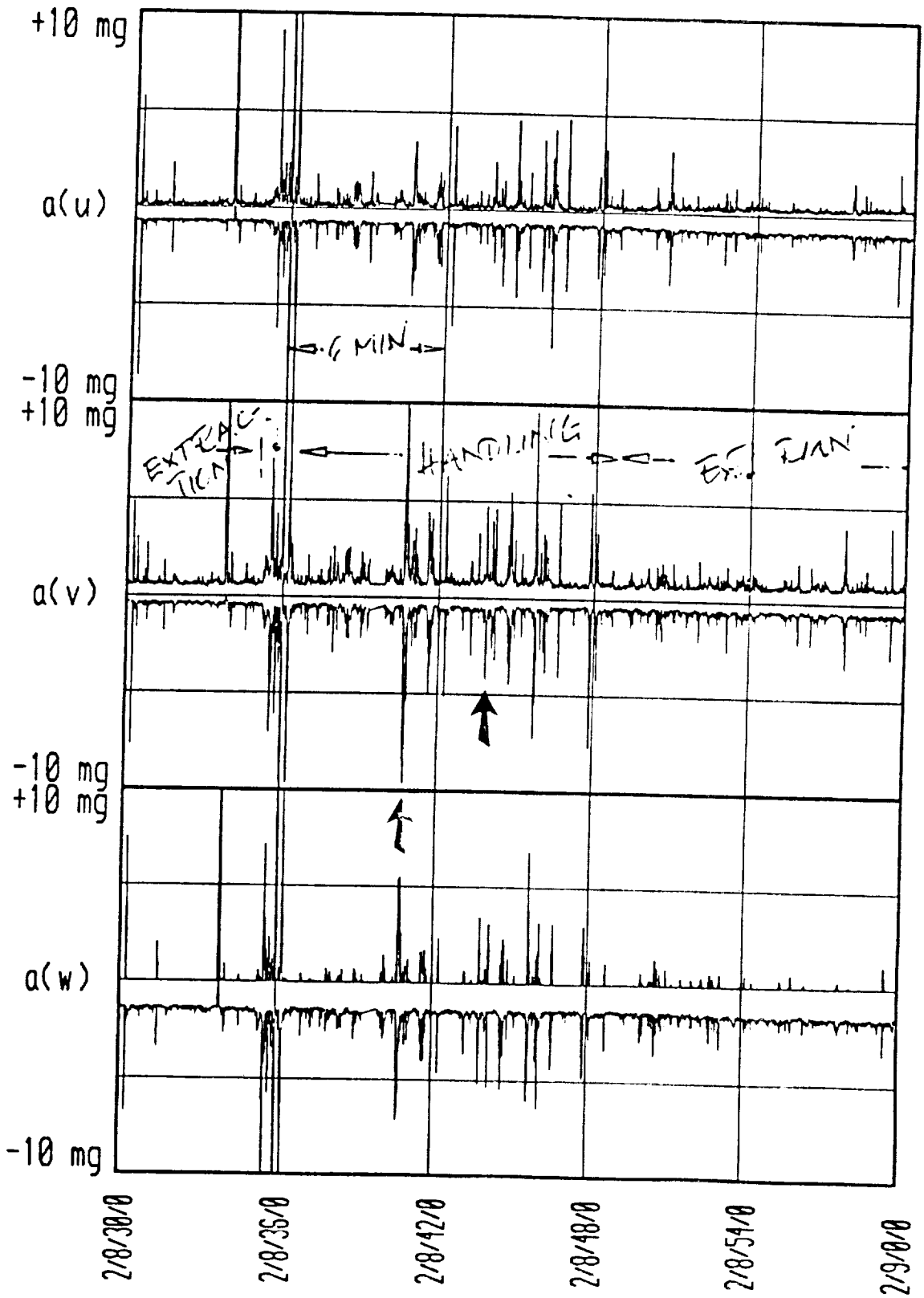

Fig. 15. FPM activities (MSDR).

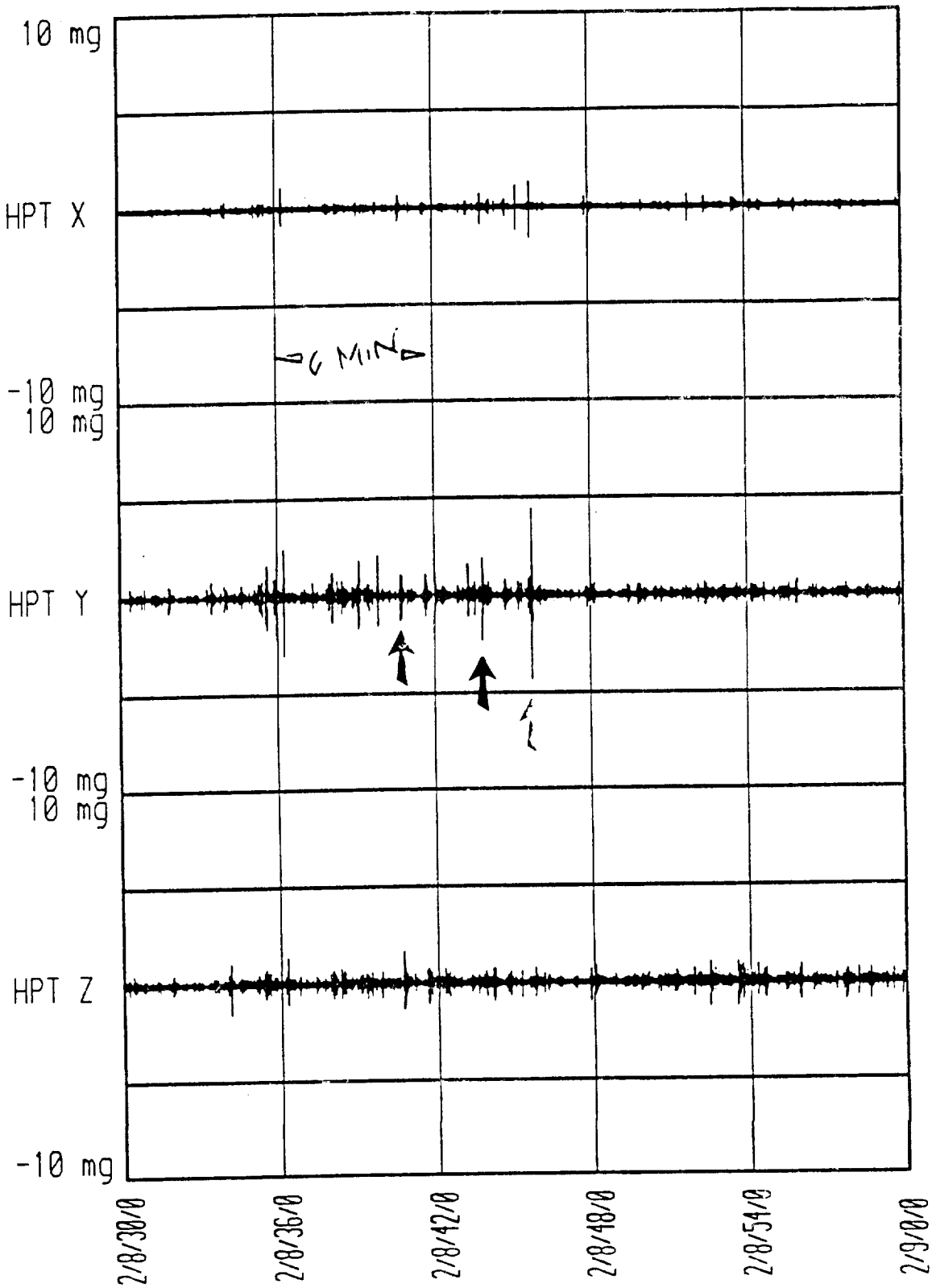

Fig.16. FPM activities of Fig.15 as detected in MEDEA.

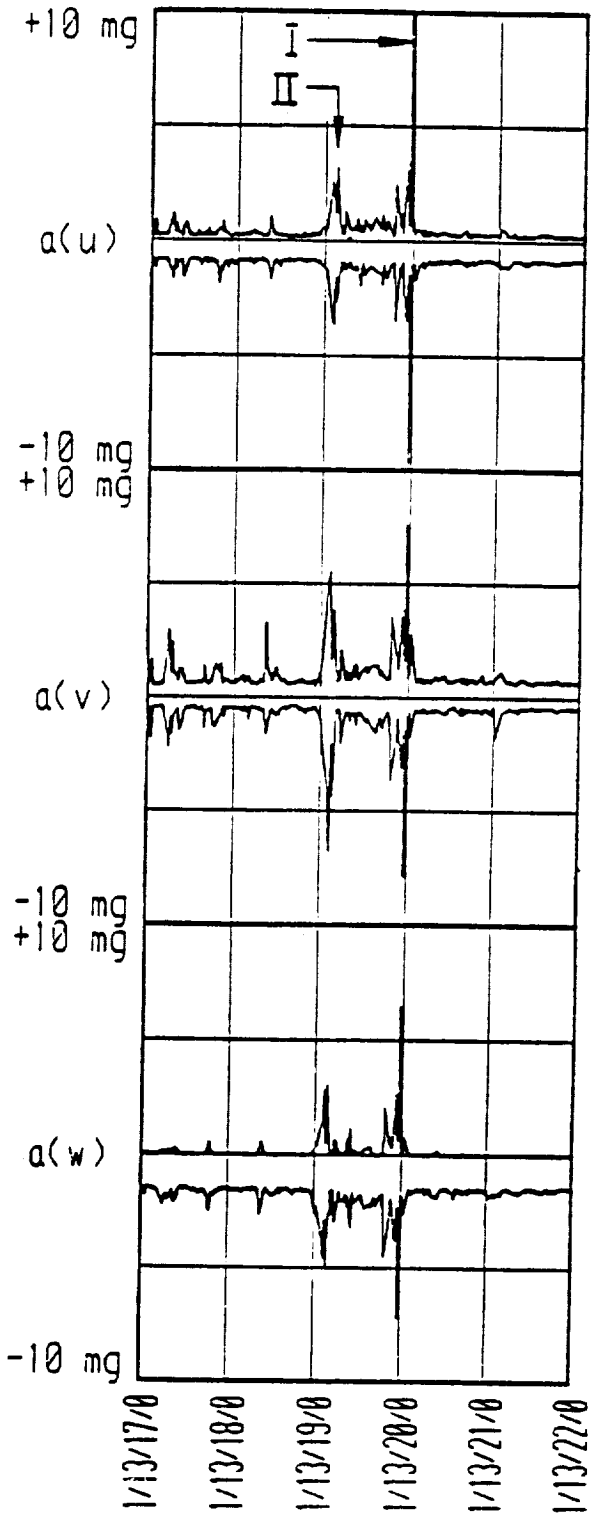

Fig.17. Examples of disturbances due to crew activities.
I Close of a container door
II Hold on the extracted FPM

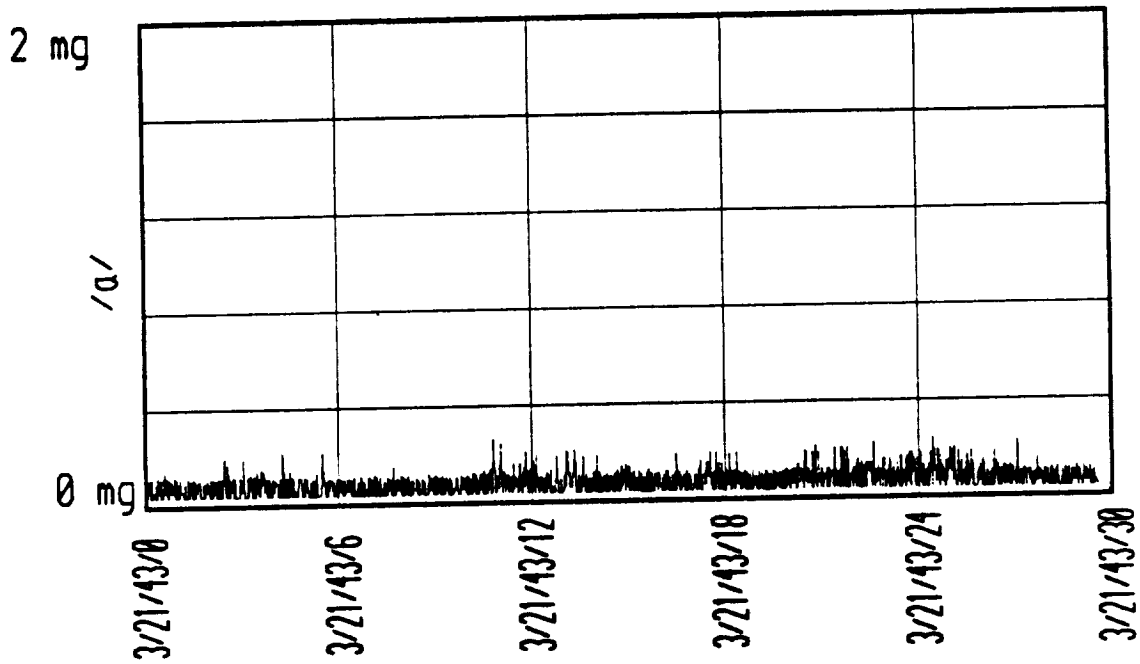

Fig.18. Example of a quiet phase. Magnitude of the resulting vector (MEDEA).

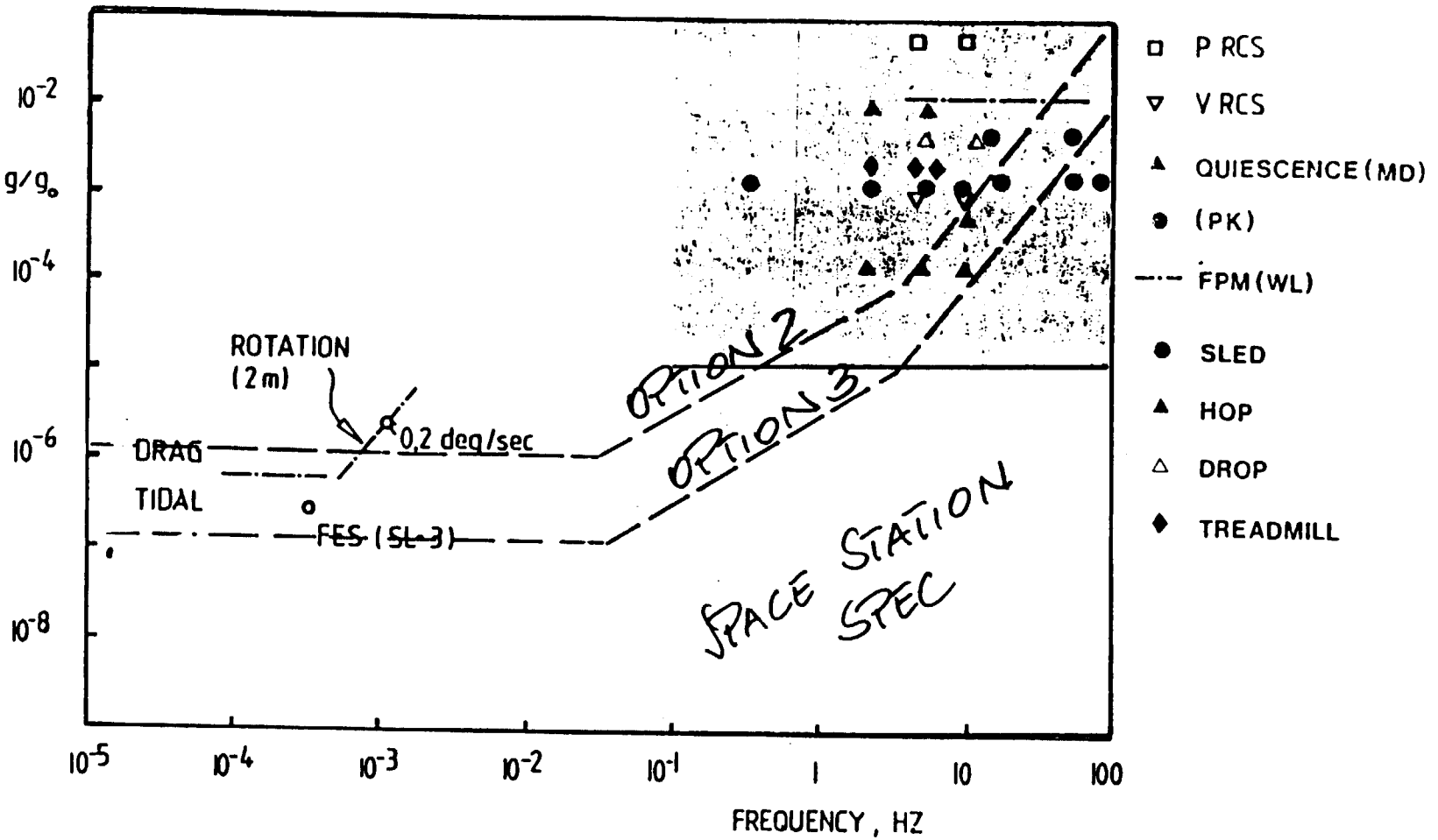

Fig.19. Summary of the measurement results.